

# Overhead Crane 2-Axis Positioning

Ryan Lederhose

June 2023

## **Abstract**

This report discusses the methodology and results surrounding developing a functioning prototype for Bluescope Steel Acacia Ridge to assist in auditing the travel path and lift rating of overhead cranes. This was achieved using the Pozyx Creator One SDK to perform the brunt of the positioning logic. An STM32 microcontroller was used to interface with a master tag, to retrieve the calculated positions, and discretise a load gauge signal used in predicting hook weight. A ZigBee network was formed to send data off the crane bridge to a host PC, where the data would then be processed and stored in a SQL database. This solution was successful at reporting the 2-axis instantaneous position and hook weight of the crane at 3.5Hz. Currently, this working prototype covers a small subsection of the warehouse; thus, a detailed recommendation plan was outlined in taking this prototype to a fully working model able to capture the position of all cranes on-site.

# Contents

<b>1</b>	<b>Introduction</b>	<b>1</b>
1.1	Motivation . . . . .	1
1.2	Background . . . . .	1
1.2.1	Pozyx RTLS Solution . . . . .	1
1.2.2	IEEE 802.15.4 . . . . .	3
1.2.3	Electronic Filters . . . . .	4
1.3	Objectives . . . . .	5
1.4	Scope . . . . .	5
1.5	Assumptions . . . . .	6
<b>2</b>	<b>Real-Time Positioning</b>	<b>7</b>
2.1	Crane 3 Layout . . . . .	7
2.2	Initial Design . . . . .	7
2.3	Positioning Accuracy . . . . .	8
2.3.1	Positioning Accuracy Tests . . . . .	9
2.4	Positioning Update Rate . . . . .	11
<b>3</b>	<b>Hook Weight</b>	<b>13</b>
3.1	Analog-to-Digital Converter Circuit Design . . . . .	13
3.1.1	Voltage Divider . . . . .	13
3.1.2	Frequency Analysis . . . . .	14
3.1.3	Time-Response Analysis . . . . .	16
3.1.4	Buffer Amplifier . . . . .	18
3.2	ADC Circuit Test . . . . .	18
3.2.1	Regression Analysis . . . . .	19
<b>4</b>	<b>External Database</b>	<b>20</b>
4.1	ZigBee Communication Test . . . . .	21
4.2	Database Storage . . . . .	22
<b>5</b>	<b>Crane 3 Implementation Test</b>	<b>23</b>
5.1	Positioning . . . . .	24
5.2	Hook Weight . . . . .	25
5.2.1	Linear Regression Model . . . . .	25
<b>6</b>	<b>Final Design</b>	<b>28</b>
6.1	System Architecture . . . . .	28
6.2	Circuit Schematic . . . . .	29
6.2.1	Microcontroller . . . . .	29
6.2.2	STLink Programming . . . . .	30

6.2.3	Master Tag . . . . .	31
6.2.4	ZigBee Module . . . . .	31
6.2.5	Analog Signal Transforming and Filtering . . . . .	32
6.2.6	Power Input and Regulation . . . . .	33
6.3	Software Architecture . . . . .	33
6.3.1	Error Checking . . . . .	36
6.3.2	Rolling Anchor Selection Algorithm . . . . .	36
6.4	Anchor and Tag Placement . . . . .	36
<b>7</b>	<b>Recommendations</b>	<b>37</b>
7.1	PCB . . . . .	37
7.2	Expanding the Coverage Area . . . . .	37
7.3	Floor Location Model . . . . .	39
7.4	Hook Weight Refinement . . . . .	40
7.5	Host PC . . . . .	40
7.6	BOM of Recommendations . . . . .	41
<b>8</b>	<b>Conclusion</b>	<b>42</b>
<b>9</b>	<b>References</b>	<b>43</b>

## List of Figures

1	Ultra-wideband Frequency versus Power Spectral Density [1] .	2
2	Open Systems Interconnection Model of Network Operation [5]	3
3	Ideal Filter Response Curves [3] . . . . .	4
4	RC Low-Pass Filter [4] . . . . .	5
5	NucleoL432KC Board to Master Tag Schematic . . . . .	8
6	21.86m x 7.6m Anchor Setup . . . . .	9
7	21.86m x 15.2m Anchor Setup . . . . .	10
8	3Hz Positioning Update Rate Test . . . . .	11
9	3.5Hz Positioning Update Rate Test . . . . .	12
10	Voltage Divider Circuit . . . . .	13
11	RC circuit with Voltage Divider . . . . .	14
12	Bode Plot of Transfer Function . . . . .	16
13	RC Circuit Time Response to 10V Input . . . . .	17
14	ADC Circuit Schematic . . . . .	18
15	Linear Regression Analysis of Table 4 . . . . .	19
16	21.86m x 45.6m Test Area . . . . .	23
17	Full Crane 3 Positioning Test . . . . .	24
18	Regression Analysis of Hook Weight . . . . .	26
19	Linear Regression Output versus Actual Mass - 2.466T . . . . .	26
20	Linear Regression Output versus Actual Mass - 3.168T . . . . .	27
21	System Architecture Flowchart . . . . .	28
22	Circuit Schematic - Microcontroller . . . . .	29
23	Circuit Schematic - STLink Programming . . . . .	30
24	Circuit Schematic - Master Tag . . . . .	31
25	Circuit Schematic - ZigBee Module . . . . .	31
26	Circuit Schematic - Analog Signal Transforming and Filtering	32
27	PCB Schematic - Power Input and Regulation . . . . .	33
28	Software Flowchart - Embedded Code for STM32 . . . . .	34
29	Software Flowchart - Host PC . . . . .	35
30	Anchor Placement for Crane 3 Expansion . . . . .	38
31	Proposed Anchor Setup for Cranes 5, 7 and 8 . . . . .	39
32	Anchor Pinout . . . . .	44
33	Tag Pinout . . . . .	45
34	Final Design Schematic . . . . .	47
35	Crane 3 Positioning Test Results . . . . .	48
36	PCB Fabrication . . . . .	49
37	Expansion to Crane 1, 3 & 15 . . . . .	50

## List of Tables

1	Technical Specifications of Crane 3 . . . . .	7
2	21.86m x 7.6m Accuracy Test . . . . .	9
3	21.86m x 7.6m Accuracy Test . . . . .	10
4	ADC Circuit Test Result . . . . .	18
5	Comparison of Wireless Communication Protocols . . . . .	20
6	ZigBee Test Range Results . . . . .	21

# 1 Introduction

The main aim of this project is to develop a functioning prototype for Bluescope Steel Acacia Ridge to assist in auditing the travel path and lift rating of overhead cranes.

## 1.1 Motivation

It has long been identified that human error is the leading cause of incidents in the workplace and thus Bluescope has always prioritised the health and safety of its workers. Bluescope Acacia Ridge has six overhead cranes on-site which are used by the operators to move steel coils. The overhead cranes pose a safety risk to the operators, and with the correct data, it is possible to introduce safety measures that would lower the risk to operators in the field.

## 1.2 Background

Bluescope have provided a real-time location system (RTLS) solution from Pozyx. The software development kit (SDK) uses anchors (stationary transceivers) to aid in positioning one or more tags (non-stationary transceivers) in a given area. Bluescope believe that with the provided software development kit, the real-time position of the overhead cranes can be captured at regular intervals. Furthermore, by integrating the real-time position with the hook weight, Bluescope can develop a heat map of the warehouse floor, indicating heavy traffic areas so appropriate measures can be introduced to reduce risks.

### 1.2.1 Pozyx RTLS Solution

The provided software development kit uses stationary transceivers, hereafter referred to as anchors, to accurately position the location of non-stationary transceivers, hereafter referred to as tags (refer to Appendix 1 for their respective pinouts). The SDK uses a positioning protocol known as Two-way-ranging (TWR).

In TWR, the distance from a tag to an anchor is measured by sending a data packet between the two transceivers. By measuring how long it took for the packet to return, the tag can estimate the distance to the anchor. If the tag has ranged with at least three anchors, it can compute its position in the given area through trilateration [2]. This consequently means the coordinates of all anchors must be known prior to positioning.

In this particular solution, one master tag instructs one or more remote tags to position themselves through the anchors. This master tag is connected to a computer or microcontroller which in turn retrieves the position from all the remote tags. Alternatively, it is possible to position the master tag itself, however, this does not scale well to large areas [2].

The anchors and tags communicate between each other through ultra-wideband (UWB) technology. UWB is a shortrange, very high frequency, wireless communication protocol that uses radio waves [1]. Consequently, UWB has problems transmitting through walls and is heavily interfered by surrounding metal. It ultimately works best if there is a clear line-of-sight between transmitter and receiver.

UWB provides a low spectral density and wide bandwidth solution to wireless communication as such:

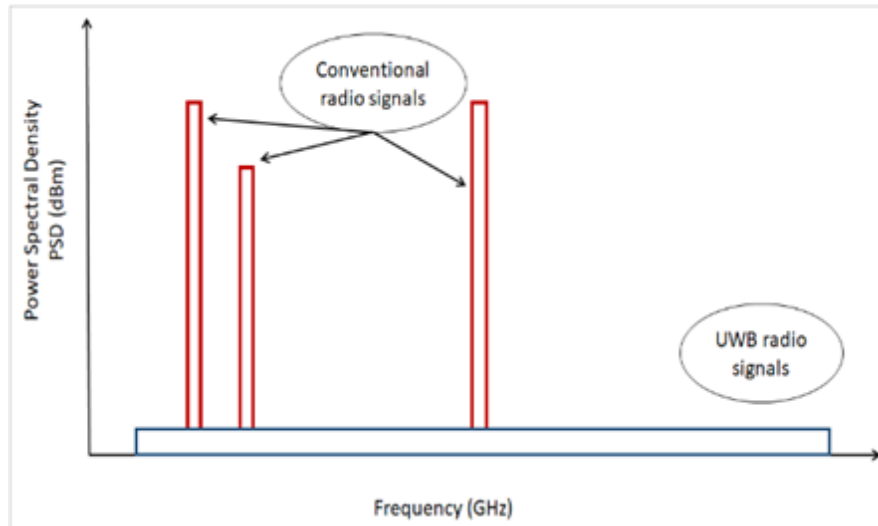


Figure 1: Ultra-wideband Frequency versus Power Spectral Density [1]

UWB features are highlighted below: [1]

- Wide bandwidth provides immunity against the channel effect, especially in a dense environment
- UWB systems can co-exist with existing narrowband systems
- UWB enables high data rates over short distances
- Low spectral density ensures low probability of signal detection and consequently increases security of connection



The Pozyx RTLS solution has four anchors and six tags, with one of these tags serving as a master tag. The master tag talks to its host device either through a serial port or an I2C connection. Pozyx claim the solution is 10cm accurate with a 60Hz update rate locally, or up to 45Hz remotely. The range of the transceivers is 30m, with Pozyx suggesting four anchors can cover a space of 400–800m<sup>2</sup>. They additionally advise a few rules be followed when placing the anchors:

1. Place the anchors high and in line-of-sight of the user
2. Spread the anchors around the user, never place them in a straight line
3. Place the anchors vertically with the antenna at the top
4. Keep the anchors away from the metal - it is advised to keep 20cm clear from the antenna to the metal

### 1.2.2 IEEE 802.15.4

IEEE 802.15 is a working group of the IEEE 802 standards committee which specifies wireless personal area network (WPAN) standards. More specifically, IEEE 802.15.4 specifies the physical layer (PHY) and media access control (MAC) layer of the Open Systems Interconnection (OSI) model of network operation.

The physical layer defines the power modulation, frequency and other wireless conditions of the link whereas the MAC layer defines the format of the data handling [5]. The standard provides a basis to which other features could be added through the upper layers. Zigbee is the most common enhancement of the 802.15.4 standard [5].

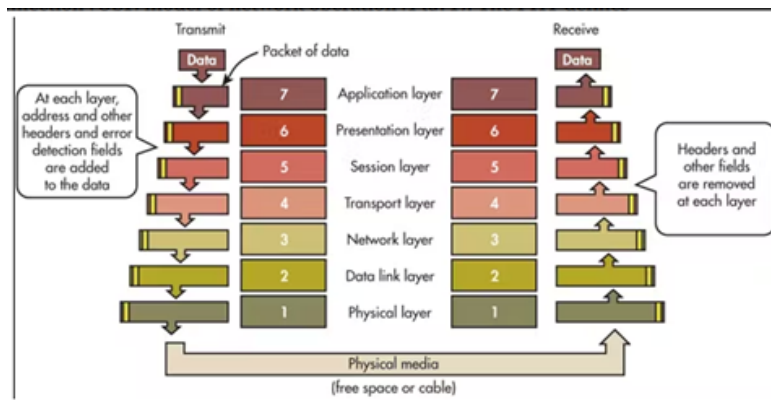


Figure 2: Open Systems Interconnection Model of Network Operation [5]

Zigbee is a mesh network protocol, which means that devices can communicate directly with each other, or they can relay messages through other devices in the network. This allows Zigbee devices to create a self-healing network that can continue to function even if some devices are out of range or out of power. There are three classes of Zigbee devices:

- Zigbee Coordinator: The coordinator forms the root of the network tree. There is always precisely one coordinator in each network since it is the device that started the network originally
- Zigbee Router: Routers can both run an application function and pass data on to other devices
- Zigbee End Device: Contains just enough functionality to talk to a router or coordinator. These devices cannot relay data and simply run an application function, fetching data and transmitting it into the mesh network

One of the key features of Zigbee is its low power consumption. Zigbee devices can run for several years on a single battery, making it well suited for use in remote or hard-to-reach locations. Additionally, Zigbee devices can operate in both sleep and active modes, which allows them to conserve power by only transmitting data when necessary.

Zigbee also has a high level of security built-in, providing data encryption and device authentication, making it a secure option for industrial and commercial applications.

### 1.2.3 Electronic Filters

Electronic filters will allow certain signals to pass through while attenuating others based on the physical architecture of the circuit. There are four major electronic filter types – low pass, high pass, band pass and band stop. Their response curves are shown below:

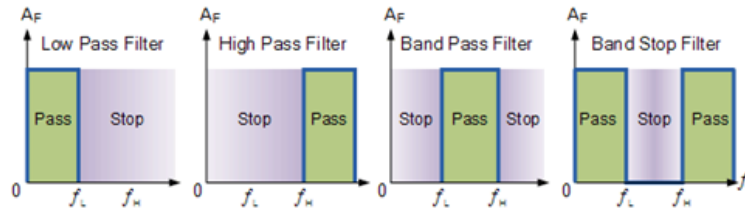


Figure 3: Ideal Filter Response Curves [3]

When converting an analog signal to a digital output via an ADC, it is important to filter the analog input with a low pass filter. A low pass filter will allow low frequencies to pass through but will attenuate the high frequencies [3] and hence by using a low pass filter on an analog input, the signal becomes less noisy, with the high frequency components being attenuated by the filter. This reduces the risk of aliasing, the phenomenon where new frequencies appear on a sampled signal after reconstruction.

A low pass filter can be constructed through a simple RC circuit:

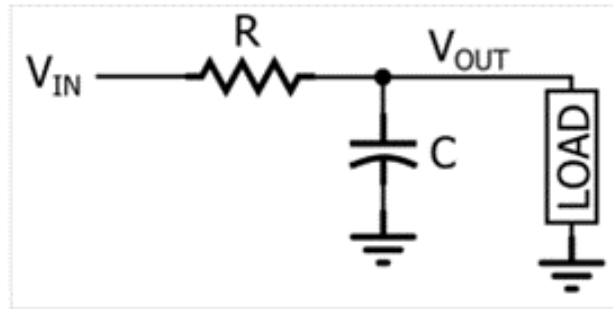


Figure 4: RC Low-Pass Filter [4]

At low frequencies, the capacitor acts as an open circuit, allowing the signal to pass to the load; however, at higher frequencies the capacitor will act as a short circuit, essentially grounding the signal. The frequency in which the circuit will begin attenuating the signal is defined as the cut-off frequency.

### 1.3 Objectives

The goal of this project is to develop a working prototype of a system capable of capturing the instantaneous 2-axis position of an overhead crane and its hook weight at periodic and synchronised units of time. The system must use the provided RTLS solution to synchronise position and weight to store in an external database with a given timestamp. The synchronised data must be repeatable for long term use. The system must be adaptable for use across all cranes on-site.

### 1.4 Scope

It is in scope of the project to:

- Determine optimal positions and number of tags and anchors for application

- Accurately retrieve position of crane hook in 2 dimensions using supplied anchors, tags and SDK
- Accurately retrieve hook weight at periodic units of time
- Synchronise data from RTLS system and weight sensor
- Develop custom software to capture hook weight and instantaneous position of the overhead crane and store in an external database at regular intervals
- Benchmark accuracy of system
- Testing of various failover scenarios and recovery (e.g. loss of database connection, loss of anchor connection)
- Develop a software test plan to test the prototype for all outcomes and scenarios using Crane 3 as a test site
- Develop a plan for a site-wide roll out of the prototype considering the different challenges for each crane

## 1.5 Assumptions

To complete this project, several assumptions had to be made:

- Load gauge attached to the cranes provides a clean 0-10V analog signal
- Bluescope will provide a method of wiring the load gauge signal
- Bluescope will provide correct power supplies
- Bluescope will cover cost of production and labour
- Bluescope will provide a method of mounting tags, anchors and necessary equipment
- A network connection will be made available

## 2 Real-Time Positioning

The scope and objective of the project requires the positioning system to meet the following requirements:

- Metre-by-metre accuracy
- Update rate great enough to capture metre-by-metre travel path of crane
- Error checking and boundary condition handling

### 2.1 Crane 3 Layout

For testing and design purposes crane 3 was used. The crane covers an area of 21.86m x 84m ( $1836.24m^2$ ). The area encompasses Bay 3, Bay 7 and rows of coil storage separating the two bays. Moreover, it is lined on the east and west sides by metal pillars, each separated by 7.6m. These pillars stretch up to the roof of the warehouse.

The crane is typically used by dispatch, to move coils from Bay 3 and the surrounding rows to Bay 7, where they will get loaded onto trucks by forklifts. In the case of wet weather, the trucks may be loaded inside the warehouse by the crane itself. The crane is also commonly used for repacking coils, where coils will be loaded onto the down-ender for turnovers by the crane.

The technical specifications for crane 3 are found in detail in the project GitHub (see Appendix 2), but are also summarised below for convenience:

Span	Height of Lift	Traverse Speed	Hoisting Speed	Long Travel Speed	Weight of Hoist	Power Supply
21.522m	9m	0.667m/s	0.0533m/s	1.0833m/s	2.5T	415V / 50Hz

Table 1: Technical Specifications of Crane 3

### 2.2 Initial Design

For an initial design a NucleoL432KC development board was used. This board uses a STM32L432KCU6 microcontroller. STM32 microcontrollers are widely supported by STMicroelectronics and the community. These microchips generally have a wide range of peripherals, including I2C, USART and ADC, making them a great option to develop firmware on. The connections between the development board and master tag are as described in Figure 5.

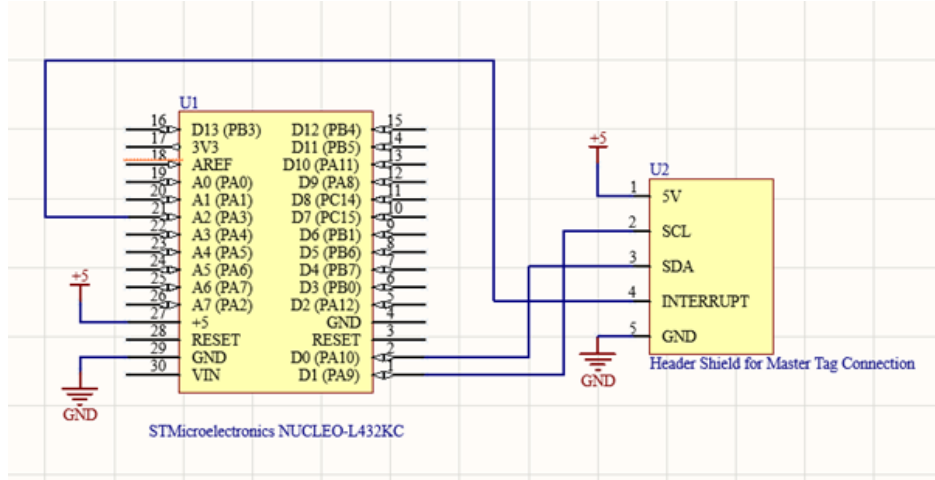


Figure 5: NucleoL432KC Board to Master Tag Schematic

## 2.3 Positioning Accuracy

The Pozyx Creator SDK offers the programmer a range of customisation options for the positioning system. These are listed below:

- Filter Options:
  - None
  - Finite Impulse Response
  - Moving Average
  - Moving Median
- Filter Strength : 1 - 15. Number of samples the position will be delayed by
- Position Dimension: 2D, 2.5D, 3D
- Position Algorithms:
  - UWB
  - Tracking

The positioning dimension is logically 2D as the scope only requires a x-y position. Hence, the positioning algorithm must be UWB, as tracking is only available in 3D positioning.

### 2.3.1 Positioning Accuracy Tests

For an initial test four anchors were used, each attached to a separate pillar 2.5m above the ground in the arrangement described by Figure 6.

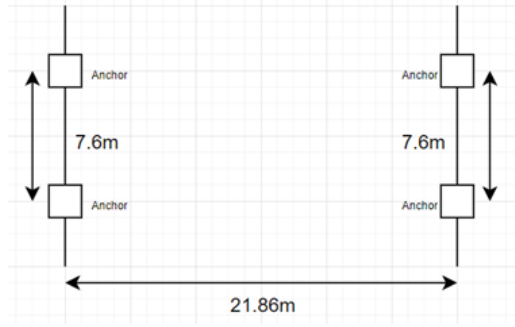


Figure 6: 21.86m x 7.6m Anchor Setup

In this arrangement, the anchors cover an area of  $166.136m^2$ . It was understood that the metal pillars would interfere with the anchor-tag transmission, however, at such short range, the effects were considered negligible.

The positioning filter was customised to a moving average filter with a strength of 10 to facilitate a smooth trajectory and a high sample rate; however, it should be noted that during this test the update rate was not considered to be a variable worth testing.

For this test, the master tag was positioned in a known location and the position calculated, which is an average over 10 results, is compared to the actual value. The results are described in Table 2.

Actual Position (mm, mm)	Calculated Position (mm, mm)	Percent Error
(1000, 0)	(990, 70)	1%
(0, 1000)	(10, 1005)	0.5%
(10900, 3800)	(10915, 3790)	0.26%
(21000, 7000)	(21048, 6950)	0.22%

Table 2: 21.86m x 7.6m Accuracy Test

Inherently, the *Actual Position* will hold some error. Taking this into account, the average percent error calculated over the test result, 0.495%, shows the positioning of the Pozyx SDK holds high accuracy and precision within the designated test area. The test area was then widened to see if the same accuracy and precision holds.

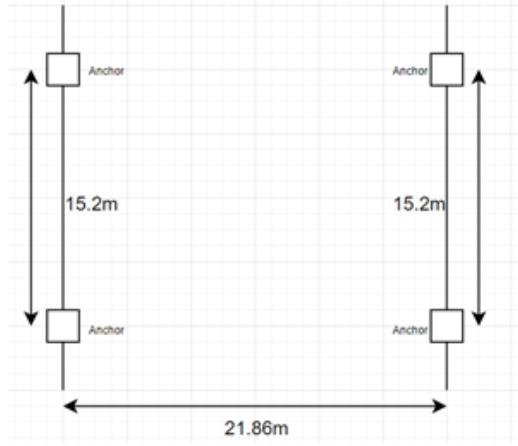


Figure 7: 21.86m x 15.2m Anchor Setup

This test introduces a remote tag to perform the positioning, to simulate an environment closer to that of the final product. The results are shown below:

Actual Position (mm, mm)	Calculated Position (mm, mm)	Percent Error
(1000, 0)	(1023, 26)	2.3%
(0, 1000)	(20, 1052)	5%
(7600, 10930)	(7892, 11334)	3.4%
(15000, 21000)	(15447, 21069)	2.9%

Table 3: 21.86m x 7.6m Accuracy Test

Expanding the test area evidently increased the percentage error in the results. This can be accounted for by the increased distance between the remote tag and the anchors. With the displacement increased, the UWB signals sent between each anchor the remote tag have a greater distance to cover. This results in the signal experiencing greater interference. It was touched on before, that the testing area is home to a large number of steel coils. These coils will interfere with the UWB communication, increasing the time it takes for the signal to reach its destination. As the Pozyx positioning protocol is based on TWR, as described before, this impacts the calculated position by the remote tag, hence why when the testing area is enlarged, the percentage error between theoretical and actual results is increased.

The scope of the project requires a metre-by-metre map of the travel path of the crane. Hence, variances in positions of up to 0.5m can be ignored



and ultimately not affect the outcome meaningfully. Thus, the increase in percentage error for this test can be considered insignificant.

## 2.4 Positioning Update Rate

The rate at which the system updates its positions should be fast enough such that a new position is calculated for every metre by the crane moves. It should be such that at least two samples are taken for every metre. This satisfies the Nyquist criterion which requires that the sampling frequency be at least twice the highest frequency contained in the signal, which in this case is the highest velocity the crane can travel. From Table 1, the long travel speed of Crane 3 is 1.08m/s at full speed (no load). Thus, accounting for disturbances, an update rate of 3Hz is sufficient.

To test this, a 3Hz update rate was implemented and the remote tag was walked around the test area as described in Figure 3. The results are as followed:

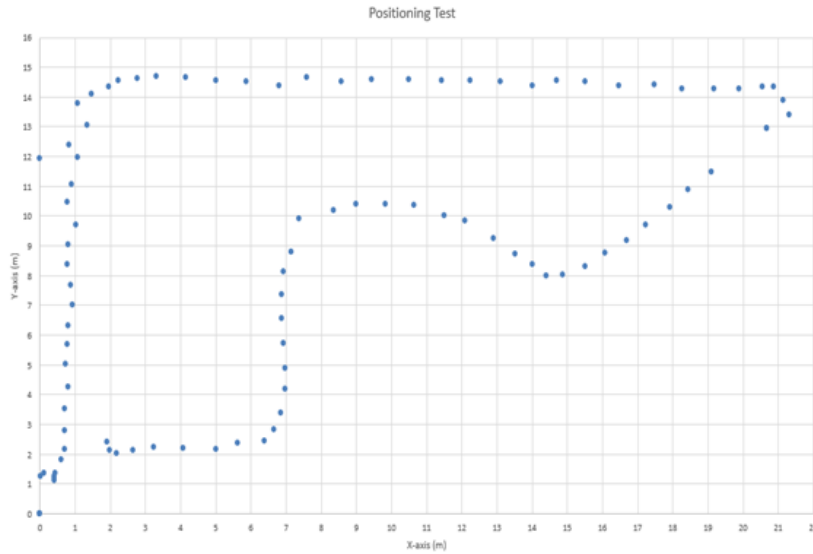


Figure 8: 3Hz Positioning Update Rate Test

Figure 8 shows that a 3Hz update rate maps the movement of the remote tag into a metre-by-metre map of the test floor. It is noticeable that the number of samples when travelling along the boundary of the x-axis is less than that when travelling along the y-axis boundary. This is not consistent when travelling along the x-axis closer to the centre of the test area. Geometrically, the centre of the x-axis boundary is cumulatively the furthest point

away from all the anchors (i.e. sum of distance to all anchors is greatest at this point). Thus, the decrease in number of samples could be accounted for by the increased distance to the anchors at this point. To account for this, the update rate was increased to 3.5Hz and the same test was conducted. The results are as followed:

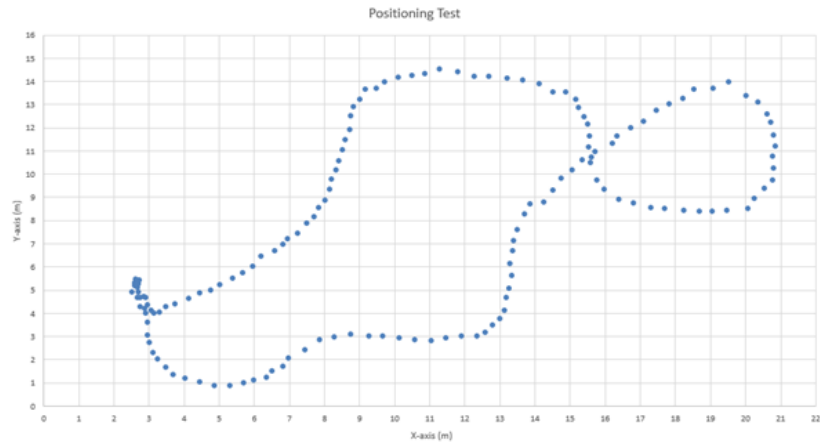


Figure 9: 3.5Hz Positioning Update Rate Test

The results of this test are much improved. There appears to be no significant decrease in the number of samples taken per metre anywhere across the floor. From these results, it can be said the 3.5Hz update rate is sufficient to track the crane to a metre-by-metre area.

### 3 Hook Weight

The load gauge attached to Crane 3 outputs a 0-10V analog signal which varies as the weight on the hook changes. Using an analog-to-digital converter (ADC), the signal can be processed and discretised, such that the hook weight can be calculated.

The scope of the project requires the hook weight be calculated at periodic intervals of time with an accuracy of 0.1T.

#### 3.1 Analog-to-Digital Converter Circuit Design

The logical choice for an ADC is on-board most STM32 microcontrollers. This eliminates the need for another IC, as well as facilitating easy configuration within the STM32CubeIDE, including configuration for a 12-bit reading. The most common input range for a single-ended ADC is 0-3.3V. Since the input from the load gauge is 0-10V, the signal must be transformed.

##### 3.1.1 Voltage Divider

To transform the voltage, a simple voltage divider was used:

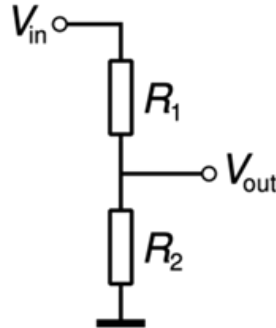


Figure 10: Voltage Divider Circuit

$$V_{out} = V_{in} * \frac{R_2}{R_1 + R_2}$$

Assuming  $R_2 = 15k\Omega$  & considering the peak voltages (i.e.  $V_{in} = 10V$ ,  $V_{out} = 3.3V$ ),  $R_1$  is then calculated:

$$\begin{aligned} 3.3 &= 10 * \frac{15 * 10^3}{R_1 + 15 * 10^3} \\ R_1 &= 30.5k\Omega \end{aligned}$$

It should be noted that  $R_2$  was assumed to be  $15k\Omega$  such that it did not draw significant current from the source. With the voltage transformed to a 0-3.3V signal, high frequency components in the signal creating noise needed to be considered.

### 3.1.2 Frequency Analysis

A low pass filter was constructed with an RC circuit, with the voltage divider forming the resistor component as such:

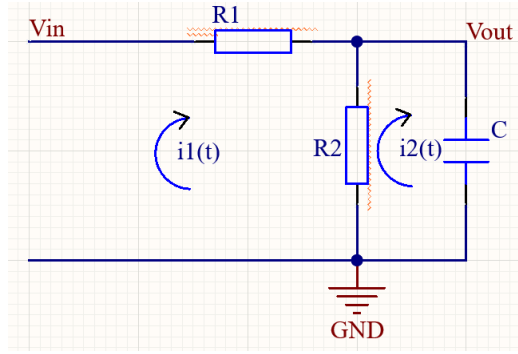


Figure 11: RC circuit with Voltage Divider

To avoid aliasing, the cut off frequency of the low pass filter should be no more than half the sample rate of the ADC. Assuming a sample rate of 2Hz, matching that of the positioning, the cut off frequency of the low pass filter will be 1Hz; Thus, the capacitance of the circuit is:

$$f_c = \frac{1}{2\pi RC}$$

$$C = \frac{1}{2\pi 15k / 30.5k} \approx 20\mu F$$

To calculate the frequency response of this circuit, the circuit can be taken to the s-domain as such:

Taking KVL for Figure 11 the following equations are yielded:

$$V_{in} = R_1 i_1(t) + R_2 (i_1(t) - i_2(t))$$

$$0 = R_2 (i_2(t) - i_1(t)) + \frac{1}{C} \int i_2(t) dt$$

$$V_{out} = \frac{1}{C} \int i_2(t) dt$$

The Laplace transform of the simultaneous equations gives:

$$V_{in}(s) = R_1 I_1(s) + R_2(I_1(s) - I_2(s))$$

$$0 = R_2(I_2(s) - I_1(s)) + \frac{1}{C_s} I_2(s)$$

$$V_{out}(s) = \frac{1}{C_s} I_2(s)$$

Writing these equations in matrix form,

$$\begin{pmatrix} V_{in}(s) \\ 0 \end{pmatrix} = \begin{pmatrix} R_1 + R_2 & -R_2 \\ -R_2 & \frac{1}{C_s} + R_2 \end{pmatrix} * \begin{pmatrix} I_1(s) \\ I_2(s) \end{pmatrix}$$

Rearranging for  $I_1(s)$  and  $I_2(s)$ ,

$$\begin{pmatrix} I_1(s) \\ I_2(s) \end{pmatrix} = \frac{1}{\Delta} * \begin{pmatrix} \frac{1}{C_s} + R_2 & R_2 \\ R_2 & R_1 + R_2 \end{pmatrix} * \begin{pmatrix} V_{in}(s) \\ 0 \end{pmatrix}$$

Where  $\Delta$  is,

$$\Delta = (R_1 + R_2)(\frac{1}{C_s} + R_2) - R_2^2$$

Solving for  $I_2(s)$  gives,

$$I_2(s) = \frac{1}{(R_1 + R_2)(\frac{1}{C_s} + R_2) - R_2^2} * R_2 * V_{in}(s)$$

$$I_2(s) = \frac{R_2 C_s}{R_1 + R_2 + R_1 R_2 C_s} * V_{in}(s)$$

Substituting in the values for  $R_1 = 30.5k\Omega$ ,  $R_2 = 15k\Omega$ ,  $C = 20\mu F$  and  $I_2(s) = V_{out}(s)C_s$ ,

$$V_{out}(s) = \frac{15 * 10^3}{15 * 10^3 * 30.5 * 10^3 * 20 * 10^{-6} s + (30.5 + 15) * 10^3} * V_{in}(s)$$

$$V_{out}(s) = \frac{15}{9.15s + 45.5} * V_{in}(s)$$

$$V_{out}(s) = \frac{1}{0.61s + 3.033} * V_{in}(s)$$

Hence, the transfer function of the system is,

$$\frac{V_{out}(s)}{V_{in}(s)} = \frac{1}{0.61s + 3.033}$$

The corresponding bode plot of the transfer function is:

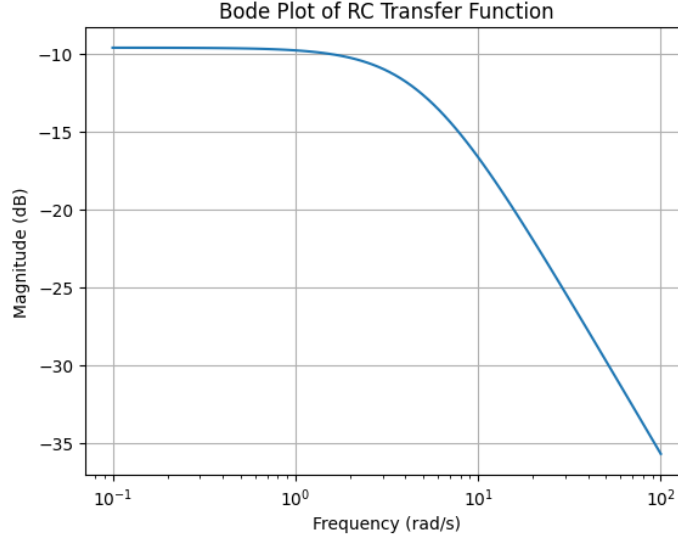


Figure 12: Bode Plot of Transfer Function

Figure 12 shows that at steady state the system experiences small attenuation,  $\approx -9dB$ , hence it can be expected that for a max input of 10V, the system will not transform the signal to a 3.3V peak, but rather bound the signal to near 3.2V due to impedance provided by the capacitor. The difference of  $\approx 0.1V$  is ultimately negligible when considering the scope of the project.

The transfer function indicates the system has one real pole at  $s = -4.972$ . This indicates that the system is:

1. Stable - Left-hand plane poles are stable, bounds the output with decaying exponential
2. Non-periodic - Complex conjugate poles result in oscillatory behaviour in the time-domain, real poles do not.

### 3.1.3 Time-Response Analysis

Assuming  $V_{in}(t) = Vu(t) \rightarrow V_{in}(s) = \frac{V}{s}$ , solving for the time-response by performing partial fraction expansion gives,

$$V_{out}(s) = \frac{1}{s(0.61s + 3.033)} * V$$

$$\frac{1}{s(0.61s + 3.033)} = \frac{A}{s} + \frac{B}{0.61s + 3.033}$$

Letting  $s = 0$  gives,

$$A = 0.32$$

Letting  $s = -4.97$  gives,

$$B = -0.2$$

Therefore,

$$V_{out}(s) = V \left( \frac{0.32}{s} + \frac{-0.2}{0.61s + 3.033} \right)$$

Taking the Inverse Laplace Transform,

$$V_{out}(t) = 0.32V (1 - 0.625e^{-4.07t}) u(t)$$

Graphing this time response to a 10V input ( $V = 10V$ ) yields the following result,

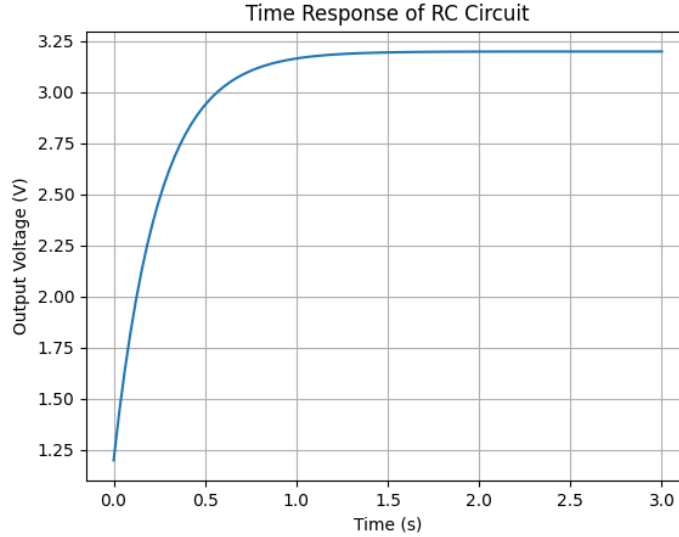


Figure 13: RC Circuit Time Response to 10V Input

As seen in Figure 13, the output voltage is bounded to  $\approx 3.24V$ , with transient response characteristics of:

- Time Constant = 0.2 seconds

- Settling Time = 0.8 seconds
- Rise Time = 0.44 seconds

The settling and rise time of the transient response is indicative of smooth and fast feedback to a step input, meeting the scope of the project.

### 3.1.4 Buffer Amplifier

The single-ended ADC input on STM32 microcontrollers typically have high input impedance of around  $40k\Omega$ . This in turn affects the analog input voltage, decreasing its magnitude. To counteract this issue, a buffer amp follows the RC circuit essentially decoupling the circuit from the ADC input. The result leads to the following schematic:

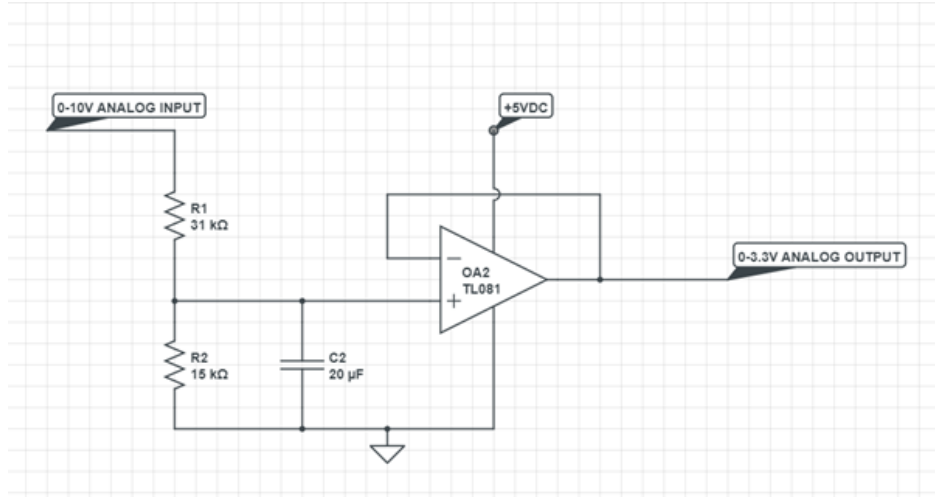


Figure 14: ADC Circuit Schematic

## 3.2 ADC Circuit Test

The ADC circuit in Figure 14 was tested using the Portacal 1000 to supply a 0-10V analog signal. The output from the buffer amplifier was wired into a single-ended ADC input on the NucleoL432KC board. The analog signal was converted by the STM32, and the digital result was pushed out to a serial port. The results from the test are as followed:

Analog Input (V)	2	4	6	8	10
Raw ADC Strain	632	1455	2265	3082	3864

Table 4: ADC Circuit Test Result



It should be noted that the raw ADC strain of each input is an average of 20 results. The variance of these results were consistently  $\leq 1$ .

### 3.2.1 Regression Analysis

Plotting the data in Table 4 and performing a regression analysis using the `sklearn.linear_regression.LinearRegression` library yields the following result:

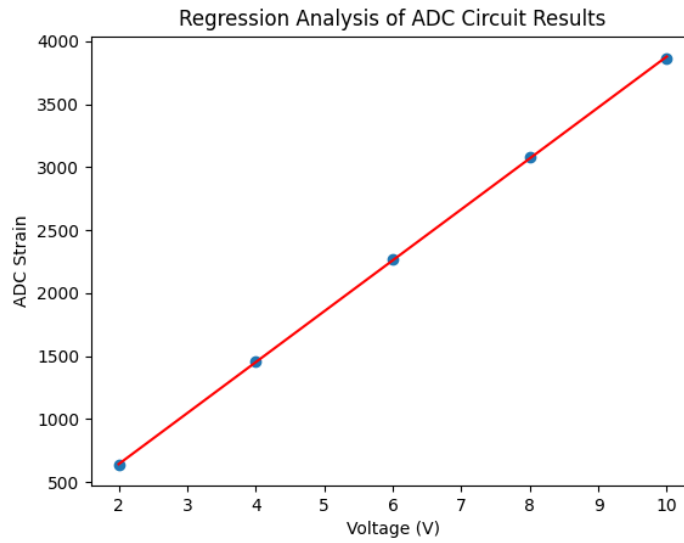


Figure 15: Linear Regression Analysis of Table 4

Predicted Function:  $y = 405.55x - 167.7$ ; Sum Squared Errors:  $SSE = 505$

According to the results of the regression analysis, there appears to be a linearly proportional relationship between ADC strain and voltage. Furthermore, the linear regression model used in the analysis was found to have a high level of accuracy, as it was able to predict ADC strains with little error. While the SSE value of 505 may seem high initially, it is important to consider the magnitude of the ADC strain in order to interpret the SSE value. In this case, when accounting for the magnitude of the ADC strain, the SSE can be seen as retrospectively low. Based on the accuracy of the model, it is possible that a similar process could be used to calculate the hook weight, although further investigation would be needed to confirm this hypothesis.

## 4 External Database

The scope of the project requires the data collected by the system be stored in an external database. However, this requires a network connection and running a wired connection to a PCB on the crane bridge is not feasible. Hence, a wireless connection is needed. The wireless connection must fulfill a list of requirements.

- Have range sufficient to reach a transmitter from crane bridge
- Have bit rates sufficient for position and mass data
  - Maximum 6 bytes for position and mass data
  - Maximum 3 bytes for crane ID → for site-wide roll out
  - At 3.5Hz update rate, 1kbps is sufficient
- Have security options available
- Be cost efficient
- Connectivity independent of external factors
- Low power consumption

The table below compres the available wireless communication protocols available:

Protocol	Range	Bit Rate	Security Options	Cost	Independence of External Factors	Power Consumption
Wi-Fi	20-40m	600Mbps	Yes	Low	No	High
Bluetooth	10m	1MBps	Yes	Low	No	High
ZigBee	0.01-1km	250kbps	Yes	Low	No	Low
Cellular Network	8-40km	45k-10Mbps	Yes	High	Yes	High
LoRaWAN	2-15km	0.3k-50kbps	Yes	Low	No	Low

Table 5: Comparison of Wireless Communication Protocols

Table 5 provides valuable information for making an informed decision on which wireless communication protocol to use. While Wi-Fi and Bluetooth offer sufficient bit rates, their limited range and high power consumption make them unsuitable for the intended purpose. Cellular networks, on the other hand, are dependent on providers and come with high costs, making them unfeasible for this project. The remaining options are Zigbee and LoRaWAN. While LoRaWAN offers a greater range, it may be too extensive

for the scope of the project. On the other hand, Zigbee’s mesh networking feature allows for seamless integration with other positioning systems, making it a highly feasible option. Therefore, based on the available information, Zigbee appears to be the most suitable wireless communication protocol for this project.

## 4.1 ZigBee Communication Test

The M5Stack Zigbee module offers a simple solution for Zigbee communication. To establish a network, a coordinator module is required to allow multiple end-devices and routers to connect and form a mesh. By connecting a coordinator module to a single-board computer (SBC) located somewhere within the warehouse, multiple end-device modules connected to positioning systems can receive positioning and weight data and push it to an external database. For this to work, the range of the Zigbee module must be sufficient to allow for long-range data transfer throughout the warehouse.

To test the Zigbee communication, an end-device module was used to send the maximum data packet (21 bytes) at a rate of 3.5Hz to the coordinator. The coordinator module was connected to a UART to USB converter, which allowed the data to be read via a host computer. The host computer was stationed in the ASL1 hut, while the end-device was taken to various locations around the site to assess the range of the Zigbee module. The results of the test are presented below:

Location	Notes
Bay 3 Door	Clean data transmission, no lost packets
Despatch Office	Clean data transmission
Bay 11	Clean data transmission
ASL5	Clean data transmission
Outside Exit Hut	Clean data transmission
Entry Hut	Some lost packets when antenna was facing South
Inside Offices	Lost packets when antenna facing away from Warehouse
Coater Rooms	Lost packets

Table 6: ZigBee Test Range Results

The results demonstrate that, with appropriate antenna placement, Zigbee communication can be achieved seamlessly throughout most of the warehouse, even at the required maximum data transfer rate. It should be noted,

however, that the tests were conducted on the ground floor where heavy interference at long range is expected. In the final design, the Zigbee modules will be placed at a higher altitude, resulting in significantly less interference than observed during these tests.

## **4.2 Database Storage**

The host computer reading the ZigBee modules incoming data will have a network connection made available. Storing the incoming data into a SQL database is the most logical option. The following parameters will be stored in the SQL database:

- Crane ID
- Update Time
- X position
- Y position
- Hook weight
- ADC count

The user will be easily filter by crane ID, and update time to query the data.

## 5 Crane 3 Implementation Test

With individual subsystems designed and tested, a full trial run with implementation on crane 3 was necessary. To simulate working conditions, the trial area was increased as below:

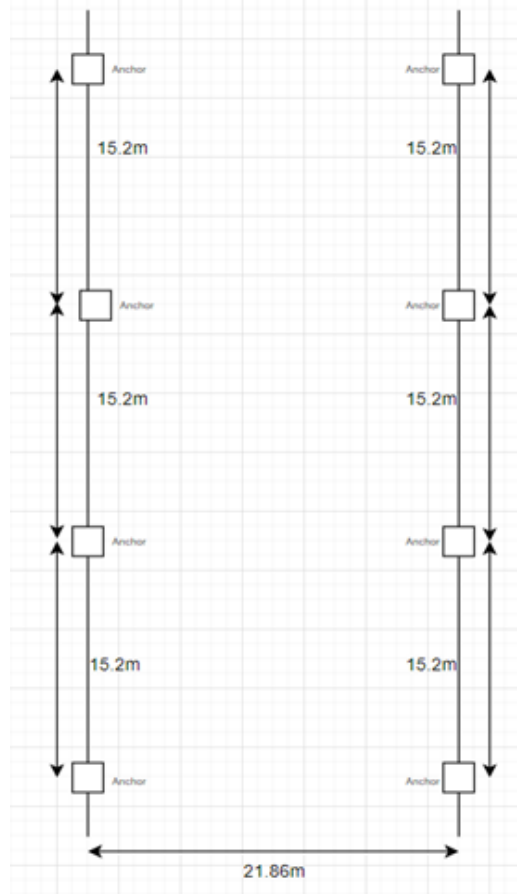


Figure 16: 21.86m x 45.6m Test Area

To expand the test area, spare tags given as part of the SDK were converted into anchors. All these anchors were placed at a height of 5m to allow sufficient range between them and the remote tag.

With integration of all 3 subsystems, it was important to upgrade the microcontroller used. The NucleoL432KC development board was substituted for a STM32L433CT6 microcontroller. The microcontroller has additional I<sup>2</sup>C, USART, SPI, and ADC ports along with an increased maximum clock frequency (80MHz). The relevant schematic for this test is located in Appendix 3.

The breadboard (containing the circuit) was secured on the crane bridge and the remote tag was connected to the crane trolley. It was important the breadboard was placed relatively central along the bridge such that the master tag and remote tag were able to maintain a consistent connection. Connections to power and the crane load gauge was left to the on-site electrician.

## 5.1 Positioning

Upon first collecting data from the crane, it was noticed that the remote tag was unable to make a connection between the two tags furthest away. Hence, to maintain a consistent connection, a *rolling anchor selection* algorithm was implemented:

```

1   if y position > 30.4m and y previous position <= 30.4m:
2       disconnect from anchors at y = 0m
3       connect to anchors at y = 45.6m
4   else if y position <= 30.4m and y previous position >
    30.4m:
5       disconnect from anchors at y = 45.6m
6       connect to anchors at y = 0m

```

Implementing this algorithm and collecting data off the crane for a 5 minute period yields the following result:

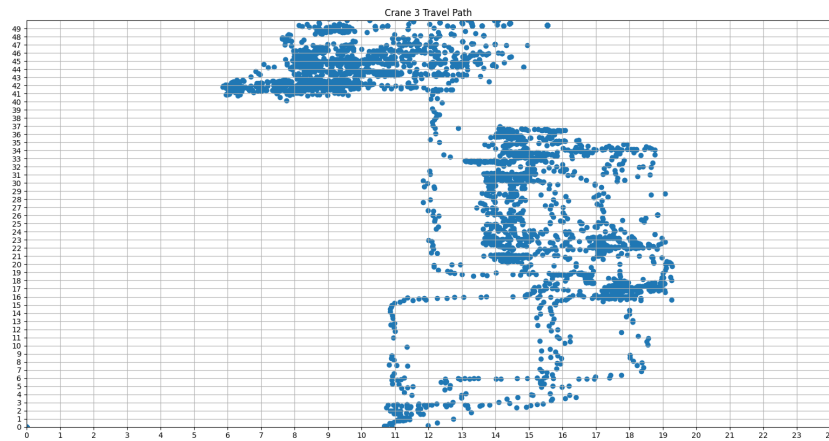


Figure 17: Full Crane 3 Positioning Test

Figure 17 illustrates some expected behavior in the crane's positioning including;

- Areas of highly concentrated data points attributed to the crane operator picking up and/or dropping off coils
- Patterns of motion beginning to outline the layout of the warehouse floor

During motion, it is evident the calculated positions show variances of  $\pm 0.5\text{m}$  on either axis. These variances are small and the scope of the project only requires a metre-by-metre map of the floor, hence they can be ignored. The features of Figure 17 indicate that the positioning system provides highly accurate and precise data. More tests were conducted in the same manner which reinforce this results (see Appendix 4).

## 5.2 Hook Weight

To test the hook weight subsystem, the ADC strain data was collected from the crane for known weight values. The data for these tests can be found in the project GitHub (see Appendix 2).

Doing a statistical analysis of the data shows the variance in the results for each weight class is  $> 5000$ . The variance initially indicates that the model will have trouble predicting the mass of a coil with high precision and accuracy due to the sensitivity of the output. Thus, the load gauge signal is not as clean as expected; however, this is out of scope for this project, hence these fluctuations can be ignored.

### 5.2.1 Linear Regression Model

By taking the average ADC strains for each mass, a linear regression model can be built to predict mass. The result is listed below:

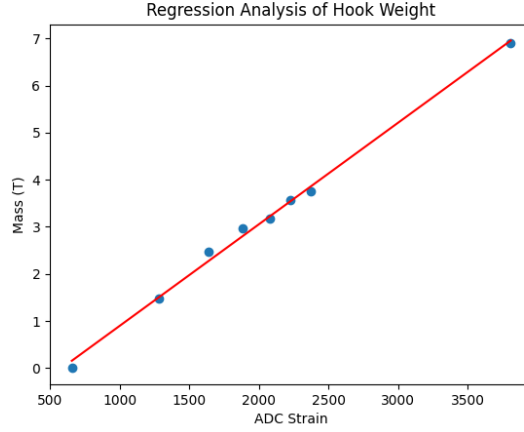


Figure 18: Regression Analysis of Hook Weight

The result of Figure 18 describes a linear regression model described by its predictive function:

$$y = 0.002159x - 1.26 \text{ (T)}$$

Using this linear regression model on testing data collected for a 2.466T coil produces the following result:

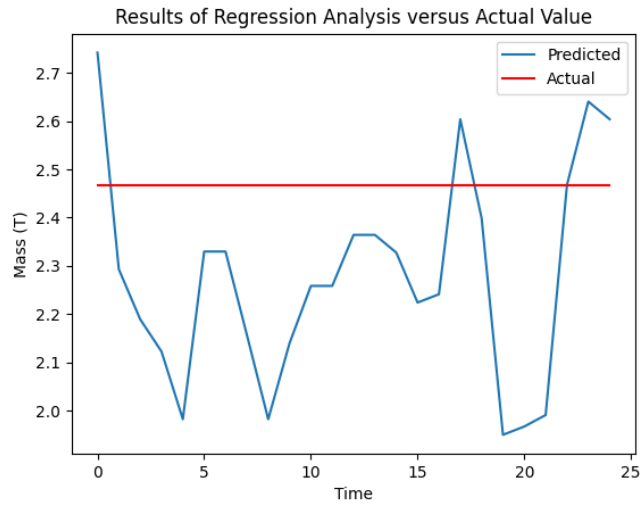


Figure 19: Linear Regression Output versus Actual Mass - 2.466T

Figure 19 shows variances in the predicted mass of up too  $\pm 0.5T$ . The squared error loss of the regression analysis is 2.055. Considering the magnitude of the output, the squared error loss indicates the model struggled to



predict with high precision. The same result holds for testing data collected for a 3.168T coil:



Figure 20: Linear Regression Output versus Actual Mass - 3.168T

Here, variances of  $\pm 0.5T$  also exist and the squared error loss is 2.07. Corresponding these variances to ADC counts show the ADC strain varies by  $\pm 200$ . Relating this back to the results obtained in 3.2, it can be concluded that the load gauge signal varies by  $\pm 1V$ .

A ML model is only as good as its training data. While it is evident that the load signal magnitude and hook weight are proportional by Figure 18, small variances in the magnitude of the signal have a large impact on the output due to its sensitivity. A linear regression model may only be a viable option if the load signal is clean.

## 6 Final Design

After the design and testing process described in Sections 2, 3, 4 and 5, a final design for the prototype was finalised.

### 6.1 System Architecture

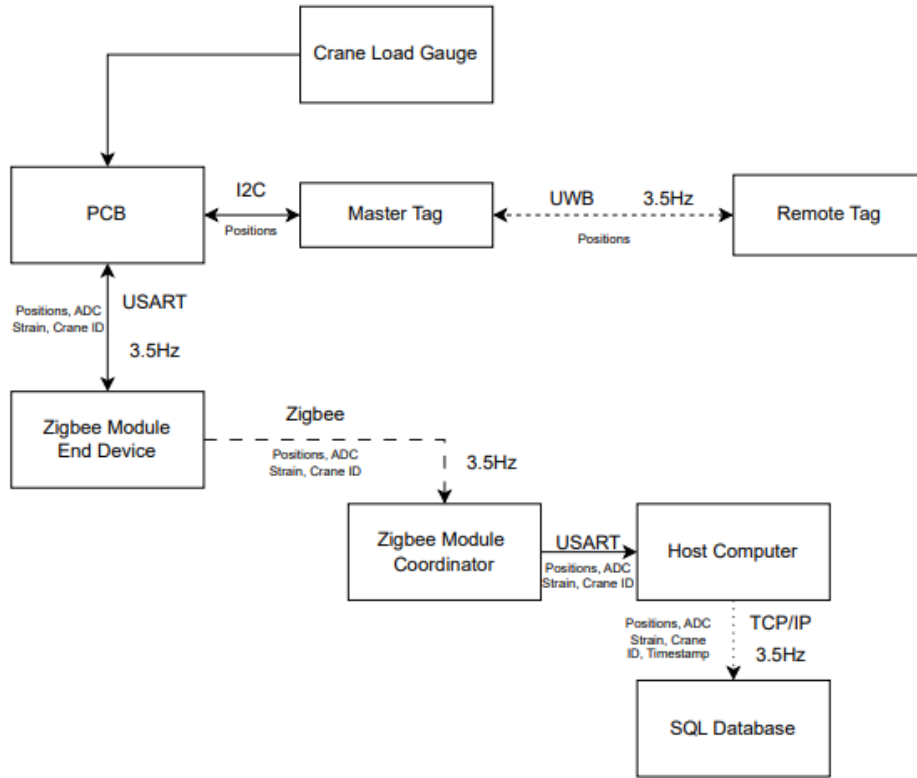


Figure 21: System Architecture Flowchart

The elements in the design are described below:

- Remote Tag - calculates position of crane
- Master Tag - communicates with remote tag to extract position of crane
- Crane Load Gauge - 0-10V signal which varies with mass on crane hook
- PCB - communicates with master tag to get positions, uses on board ADC to get ADC strain of load gauge, does relevant error checking, sends data to end device

- ZigBee End Device - to send positions, mass and crane ID to coordinator at 3.5Hz
- ZigBee Coordinator - to receive data from end devices and relay to a host computer
- Host Computer - to read data from ZigBee Coordinator and send to SQL database
- SQL Database - to store data in a safe and secure location

## 6.2 Circuit Schematic

The circuit schematic can be broken down into 6 different subsystems, each with an important role.

### 6.2.1 Microcontroller

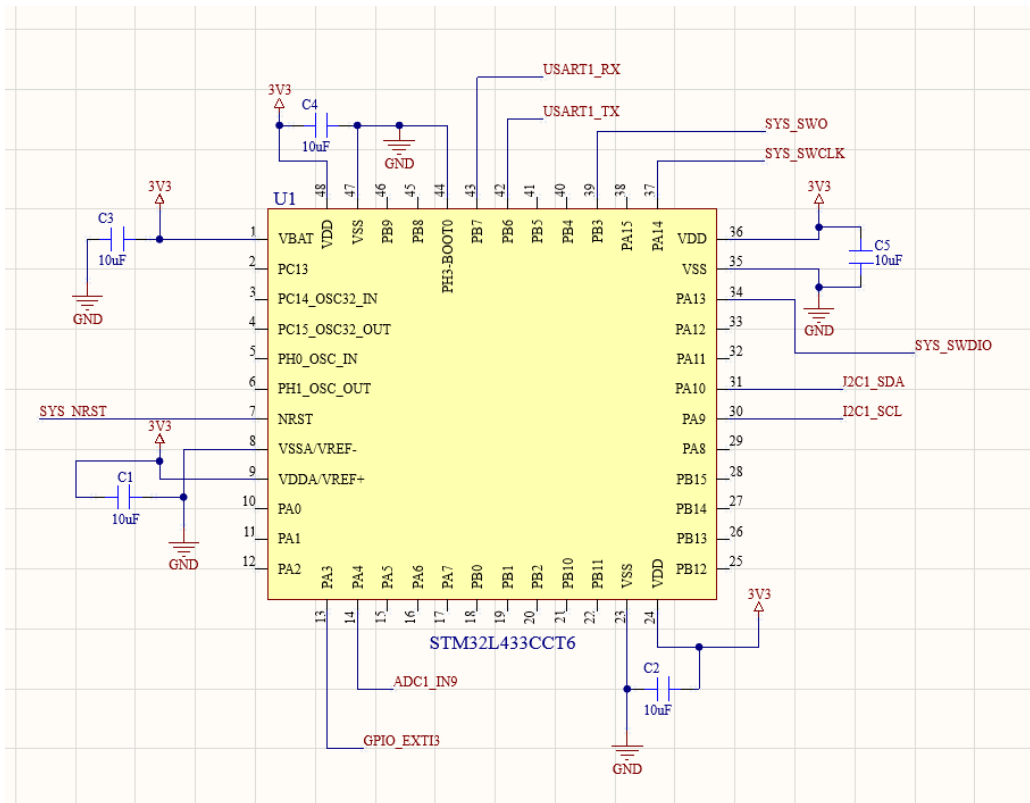


Figure 22: Circuit Schematic - Microcontroller

The chosen microcontroller is the STM32L433CCT6, hereafter referred to as the MCU. Key features of the MCU relevant to this project include:

- Ultra low-power - 1.71-3.6V supply
- 32-bit ARM Cortex
- 3 x I<sup>2</sup>C buses
- 4 x USARTs
- 1 x 12 bit ADC
- 256kB flash
- NVIC
- Surface-Mount
- 9mm by 9mm
- Low cost - \$10.87

The MCUs ultra low power requirements made it a standout choice as power is a scarce resource on the crane bridge. Its rich supply of communication and GPIO ports add to its feasibility. The power pins are fed a 3.3V signal and 10 $\mu$ F decoupling capacitors are used for reliable power consumption. The MCU is flashed via the STLink Programming subsystem.

### 6.2.2 STLink Programming

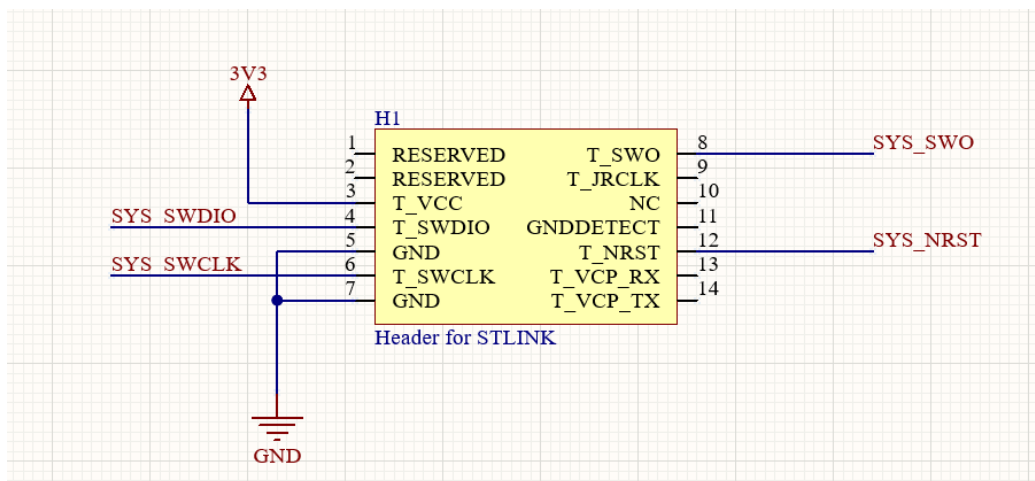


Figure 23: Circuit Schematic - STLink Programming

The MCU is programmed via the *STLINK-V3MINIE* (\$18.25).

### 6.2.3 Master Tag

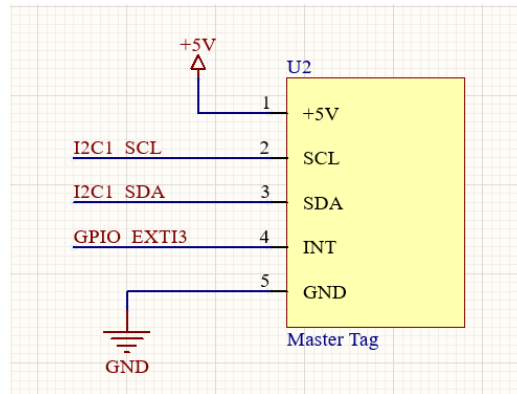


Figure 24: Circuit Schematic - Master Tag

The master tag talks to the MCU via an I<sup>2</sup>C port.

### 6.2.4 ZigBee Module

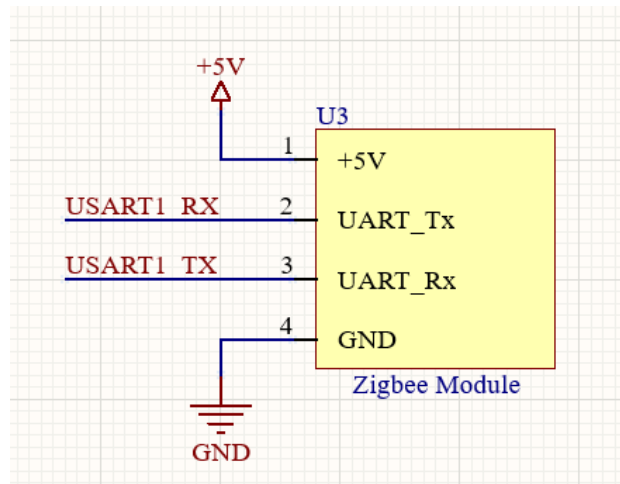


Figure 25: Circuit Schematic - ZigBee Module

The ZigBee modules used are the *Zigbee Unit (CC2630F128) with Antenna* provided by M5Stack. A flexicable is used between the circuit and the module.

These ZigBee modules were used in the testing stage and proved they could sustain a reliable connection across majority of the warehouse floor.

### 6.2.5 Analog Signal Transforming and Filtering

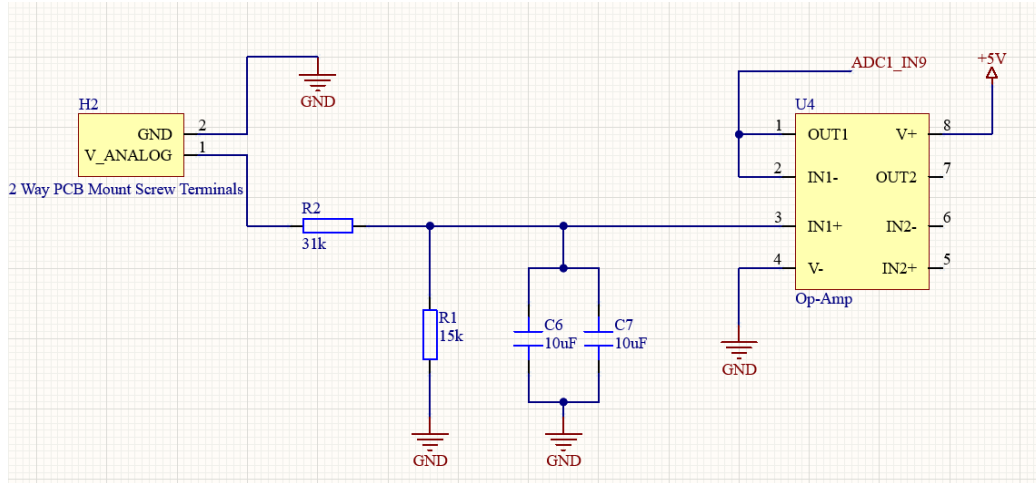


Figure 26: Circuit Schematic - Analog Signal Transforming and Filtering

This part of the circuit is built as described by Section 3. To receive an analog signal from the crane load gauge, a two-way screw terminal is used, which allows a secure and safe connection. This input is passed through an RC circuit, which caps the voltage to 0-3.3V, and filters out any unwanted high frequency noise. Then an op amp, configured as a voltage follower, facilitates an electrical connection between this circuit and the MCU such that the high input impedance of the ADC does not impact the signal. The op-amp chosen for use in the circuit is the [LM358](#), manufactured by TI.

### 6.2.6 Power Input and Regulation

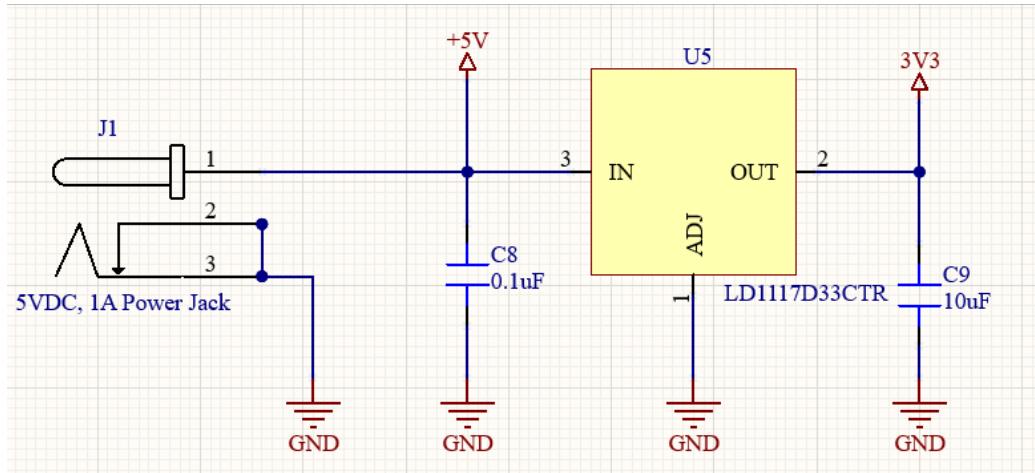


Figure 27: PCB Schematic - Power Input and Regulation

A 5V, 1A (5W) DC power plug is used to supply power to the board. A [LD1117](#) voltage regulator, is used to regulate the voltage to 3.3V, supplying a 800mA current.

## 6.3 Software Architecture

The software for the prototype is split up into two parts: embedded code for STM32 and software for host PC:

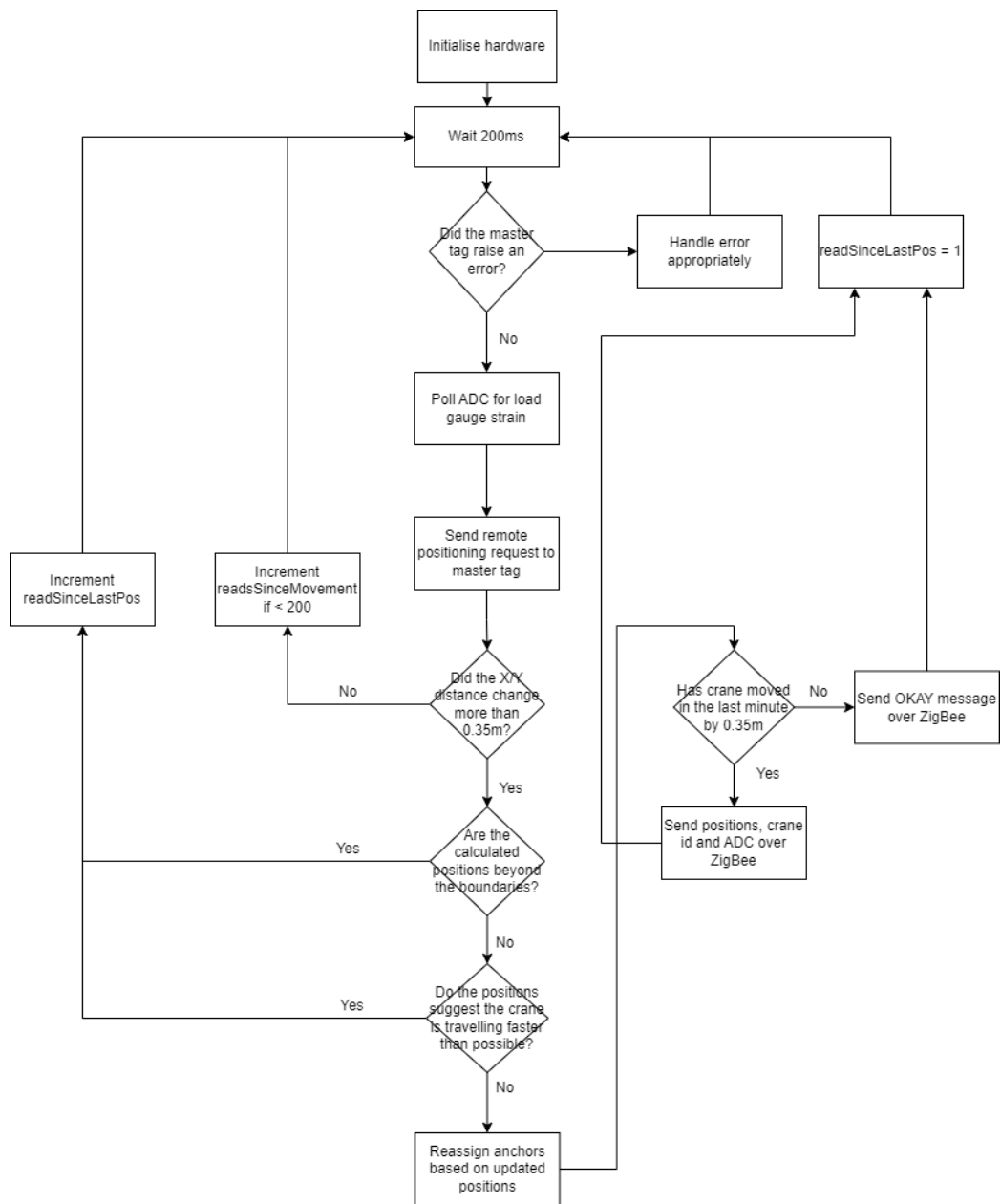


Figure 28: Software Flowchart - Embedded Code for STM32

Key actions taken in Figure 28 include:

- Position filter and strength set to moving average and 10 respectively
- Register settings and anchor selections of master and remote tag flashed to memory in case power is lost



- Turned off on-board sensors on the tags
- Error checks
- ADC polling
- Positioning requests

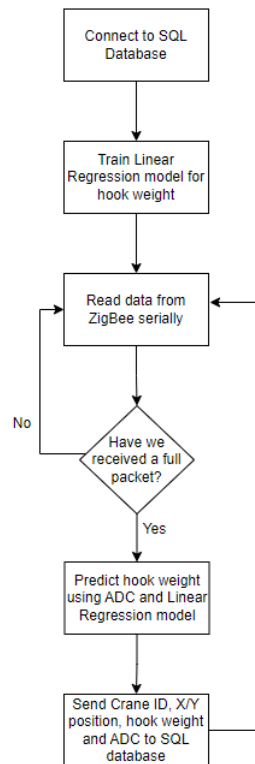


Figure 29: Software Flowchart - Host PC

Key actions taken in Figure 29 include:

- Train ML model for hook weight prediction
- Initialise connection to SQL database
- Read data serially from ZigBee coordinator and establish if a full packet has been received yet
- Parse packet to send to SQL database

### 6.3.1 Error Checking

Errors are handled appropriately in the code. Errors considered regarding positioning include:

- Positions outside boundaries
- Positions suggesting crane is moving faster than possible

When these errors are detected, the software will ignore this measurement and restart the cyclic executive. For errors associated with master tag, an interrupt indicates to the software that something has gone wrong. Errors considered and their appropriate action plan include:

- Error in Positioning → request position again
- Loss of Connection with Remote Tag → raise error with database, try reconnection
- Loss of Anchor Connection → raise error with database, try reconnection

### 6.3.2 Rolling Anchor Selection Algorithm

Due to range limitations in UWB, a rolling anchor selection algorithm had to be implemented. This was discussed and tested in Section 5.1.

## 6.4 Anchor and Tag Placement

Anchors are placed as shown in Figure 16 at a height of 5m. The remote tag is attached to the crane trolley and the breadboard (circuit) is mounted centrally on the crane bridge.

## 7 Recommendations

The prototype is currently designed for a small subsection of the warehouse. To take this prototype to a model capable of being used across site, there are multiple changes/actions that should be taken.

### 7.1 PCB

Manufacturing PCBs is a logical next step for site-wide deployment. Using the current circuit schematic a PCB was designed (see Appendix 5 for fabrication). While this PCB would be sufficient, it could be optimised. The main disadvantage surrounding this PCB is that the ZigBee module is external. This means the system is not overly compact. To rectify this issue, research would have to be conducted on appropriate ZigBee solutions that could be soldered onto the PCB.

Key design choices of the PCB include:

- Master tag is intended to sit on top of PCB keeping design compact while avoiding any unnecessary 'flying' wires
- Regions near UWB antenna kept clear of electronics
- Two-way screw terminal for load gauge signal attached to bottom of PCB
- 5W DC power plug used to provide power

For 10 of these PCBs, JLC charges \$10AUD. Please refer to the project GitHub (see Appendix 2) for a full BOM of the electrical components. The cost of the components for a single PCB comes to \$54.84AUD, hence, for deployment on all 6 cranes, the cost of the PCB and components comes to \$345.22AUD.

### 7.2 Expanding the Coverage Area

To expand the coverage area, more anchors are needed. For crane 3, if anchors were placed on every other pillar, as done in the testing phase, 14 anchors would be needed. This is shown below in Figure 30:

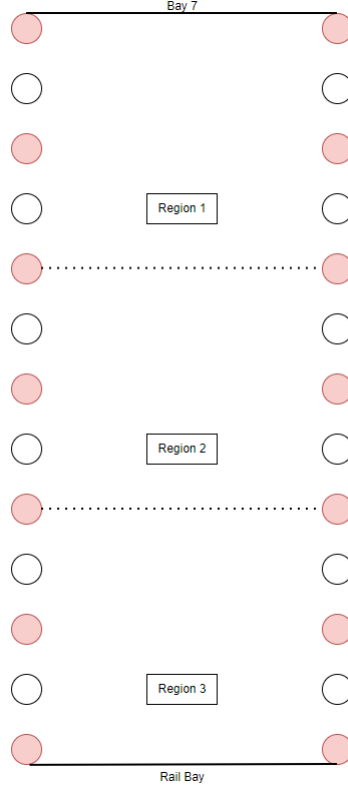


Figure 30: Anchor Placement for Crane 3 Expansion

In Figure 30, circles represent the pillars in the bay, and the red fill represents anchors attached to these pillars. Furthermore, three regions are outlined, each one specifying a different area of space for which the *rolling anchor selection* algorithm identifies to appropriately assign active anchors for positioning. Theoretically, this expansion should be seamless.

Expanding to crane 1 and 15 follows a similar approach taken above (see Appendix 6 for layout). The difference here is that crane 1 uses shared anchors between crane 15, on its west side, and crane 3, on its east side. Its unknown if using this shared anchor approach has any effect on the latency (or even accuracy/precision) of the results; however, theoretically, Pozyx suggest this should be seamless. The obvious advantage of this approach is the cost savings, cutting the number of anchors from 42 to 28, so it is worth investigating.

Crane 5 is lined by 10 pillars on the north side; however, on the south side it is lined by only 5 pillars and a metal wall. Placing anchors on the north side is simple enough, however, issues may arise mounting anchors on the metal wall. Moreover, it is unknown how this wall may impact transmis-

sion between the anchor and tag. Crane 7/8 shares its north side with crane 5; hence, only 2 shared anchors is possible. Unfortunately, cranes 7 and 8 share space with heavy infrastructure from the paintline, hence it may prove difficult to maintain consistent connection with these anchors ultimately impacting the latency and accuracy/precision of the results. Figure 31 show this proposed anchor setup:

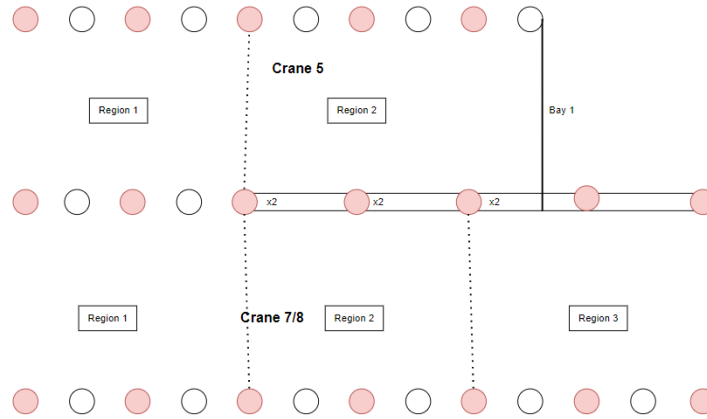


Figure 31: Proposed Anchor Setup for Cranes 5, 7 and 8

It is recommended that all anchors are placed at a height of 5m. The remote tag should be attached to the crane trolley, while the master tag and PCB is mounted centrally on the crane bridge. These approaches showed success in the testing phase.

The project GitHub has a full layout of the proposed anchor layout for the site. For a sitewide roll out it will require:

- 50 anchors
- 6 tags

This comes to a total cost of \$21,720.15AUD (including the price of the already received SDK).

### 7.3 Floor Location Model

Extracting the floor location of the crane based on the position would provide meaningful abstraction to the data. This could be done through a simple k-Nearest Neighbours ML model. This could be implemented on top of the host PC software and should provide no disadvantages as far as computational expenses go. While implementation is relatively simple, extracting the

training data required could be expensive, especially in areas with a dense number of defined floor locations. Hence, building this model is a trade-off between time and meaningful data abstraction.

## 7.4 Hook Weight Refinement

The hook weight calculation system is built on top of training data collected from various weights. To improve the prediction when implementing this product site-wide, more training data should be collected. Furthermore, to improve the precision of the results, the load gauge signals should be relatively noise free as the effect of noisy signals was seen in Section 5.2.

## 7.5 Host PC

The prototype requires a USB connection to a UART-USB converter to read the output from the ZigBee coordinator module. While this works, it definitely could be more efficient. It is recommended that the host PC is moved to a single board computer. Usually, these SBCs provide UART pins, removing the need for the UART-USB converter, and supply a network connection, over wifi or ethernet (or both). Furthermore, the size and power requirements of SBCs provides extreme versatility over a regular computer/laptop. While the Raspberry Pi 3 or 4 is the obvious choice, supply issues make it difficult to get one, hence alternatives need to be considered. Standout choices after research are the [Raspberry Pi Zero W](#) and the [AML-S905X-CC \(Le Potato\)](#). Differences between the two models are described below:

- Cost: Le Potato 2GB - \$60AUD, RPi Zero W - \$20AUD
- Network Connection: Le Potato 2GB - WiFi and Ethernet, RPi Zero W - WiFi
- RAM: Le Potato - 2GB, RPi Zero W - 512MB
- OS: Both can run any linux distro

On top of this, the Le Potato is form factor compatible with the Raspberry Pi 2 or 3.

The aim of the host PC is simple - read data from ZigBee module, predict the hook weight and send to SQL database. These processes aren't overly computationally expensive, thus the 512MB RAM on the RPi Zero W should be sufficient. The deal breaker between these two models is hence the cost and network connection. While the ethernet compatibility and process speed of the Le Potato trumps the RPi Zero W, it could be considered over kill for

its purpose. Hence, the RPi Zero W appears to be the more sensible solution; however, both proposed models are acceptable.

## 7.6 BOM of Recommendations

The cost of the proposed recommendations for site-wide deployment comes to:

- Anchors and Tags - \$21,720.15AUD
- PCB and Components - \$345.22AUD
- Raspberry Pi Zero W - \$20AUD
- **Total Cost  $\approx$  \$22,000AUD**

## 8 Conclusion

The goal of this project was to develop a working prototype of a system capable of capturing the instantaneous 2-axis position of an overhead crane. Through a rigorous testing phase, this goal was met. The Pozyx Creator One SDK was used to capture the position of a remote tag located on the crane trolley. A master tag transmitted this position to a MCU (STM32) over I2C. Furthermore, the MCU discretised a load gauge signal used to capture the hook weight. A ZigBee network connection was used to transmit data off the crane bridge to a host PC, where it would process the data (predict hook weight) and send to an external SQL database for storage. A detailed plan of future recommendations was outlined, which would cost the company  $\approx$  \$22,000AUD. Ultimately, it could be said that this project was a success.



## 9 References

- [1] M.Bakr. "Introduction to Ultra-Widband (UWB) Technology". All About Circuits. <https://www.allaboutcircuits.com/technical-articles/introduction-to-ultra-wideband-uw-b-technology/>
- [2] "Positioning protocols explained". Pozyx Academy. <https://www.pozyx.io/pozyx-academy/positioning-protocols-explained/>
- [3] W.Storr. "Passive Low Pass Filter". Electronics-Tutorials. [https://www.electronics-tutorials.ws/filter/filter\\_2.html](https://www.electronics-tutorials.ws/filter/filter_2.html)
- [4] R.Keim. "What is a Low Pass Filter? A Tutorial on the Basics of Passive RC Filters". <https://www.allaboutcircuits.com/technicalarticles/low-pass-filter-tutorial-basics-passive-RC-filter/>
- [5] L.Frenzel. "What's The Difference Between IEEE 802.15.4 and ZigBee Wireless?". <https://www.electronicdesign.com/technologies/wireless/article/21796046/whats-the-difference-between-ieee-802154-and-zigbee-wireless/>
- [6] "How ultra-wideband works". Pozyx Academy. <https://www.pozyx.io/pozyx-academy/how-does-ultra-wideband-work/>
- [7] "Ultra-wideband and obstacles". Pozyx Academy. <https://www.pozyx.io/pozyx-academy/ultra-wideband-and-obstacles/>
- [8] "Creator". Pozyx Creator Documentation. <https://docs.pozyx.io/creator/>

## Appendix 1: Anchor and Creator Tag Pinout

### Anchor Pinout

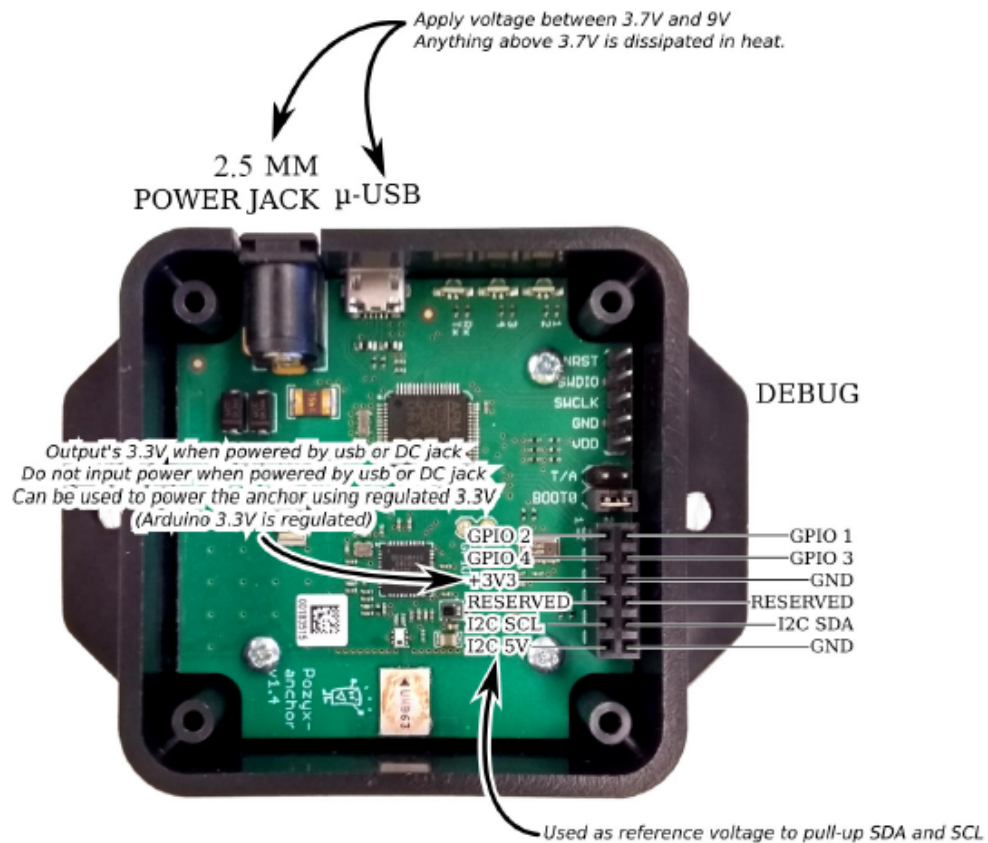


Figure 32: Anchor Pinout



## Appendix 2: Important Links

1. [Overhead-Crane-Real-Time-Location-System GitHub Page](#)
2. [Pozyx Creator One Kit](#)
3. [Pozyx Creator One Documentation](#)

## Appendix 3: Final Design Schematic

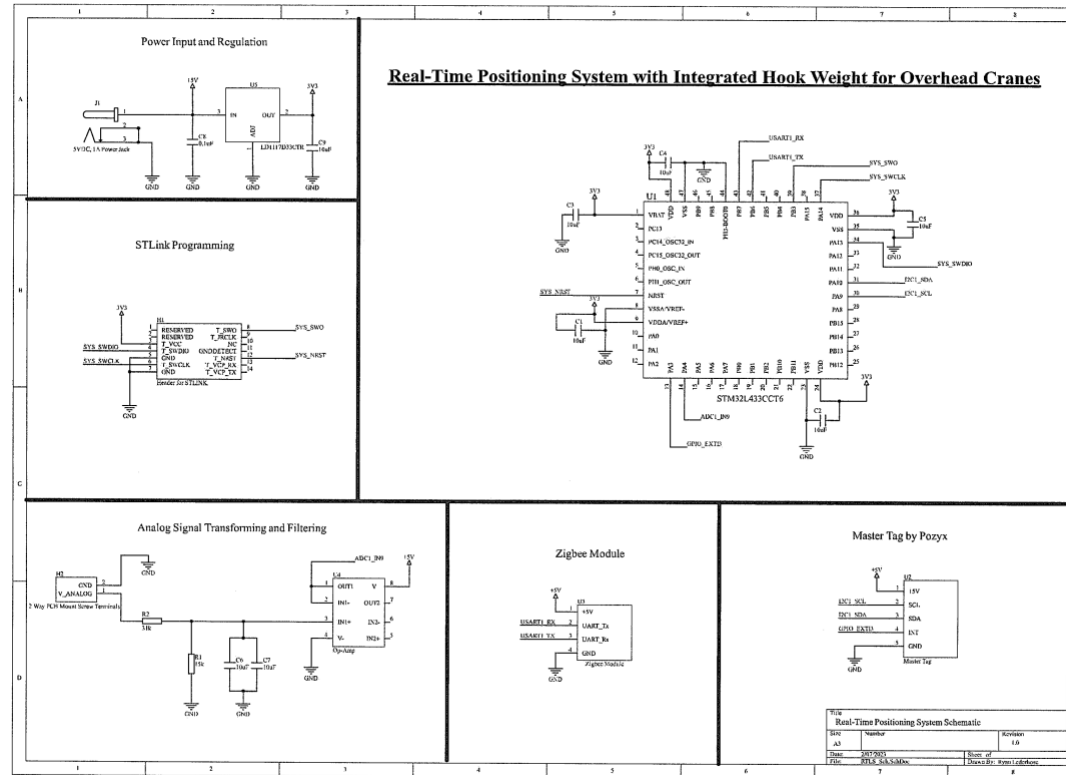


Figure 34: Final Design Schematic

## Appendix 4: Crane 3 Positioning Test Results

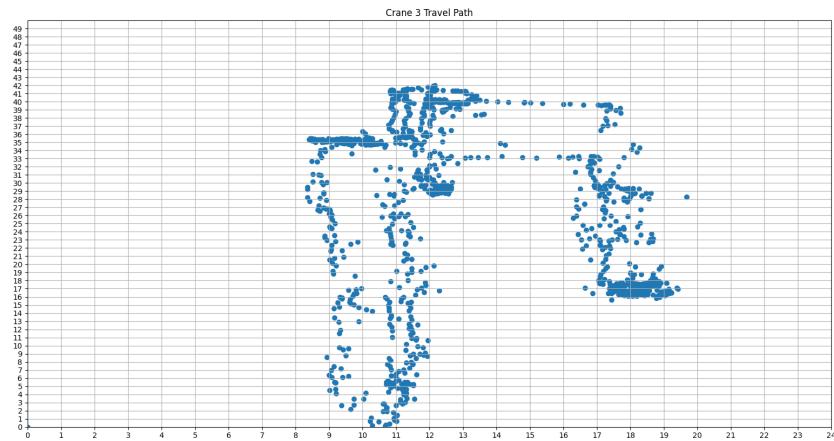


Figure 35: Crane 3 Positioning Test Results

## Appendix 5: PCB Fabrication

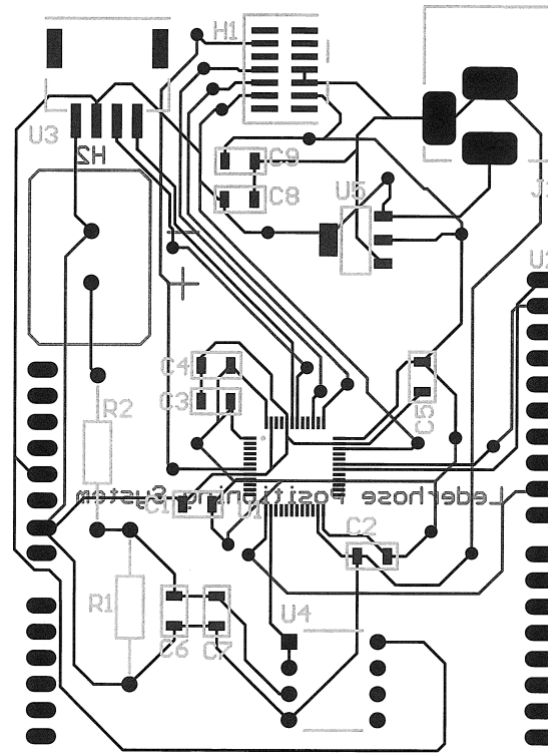


Figure 36: PCB Fabrication

## Appendix 6: Expansion to Crane 1, 3 & 15

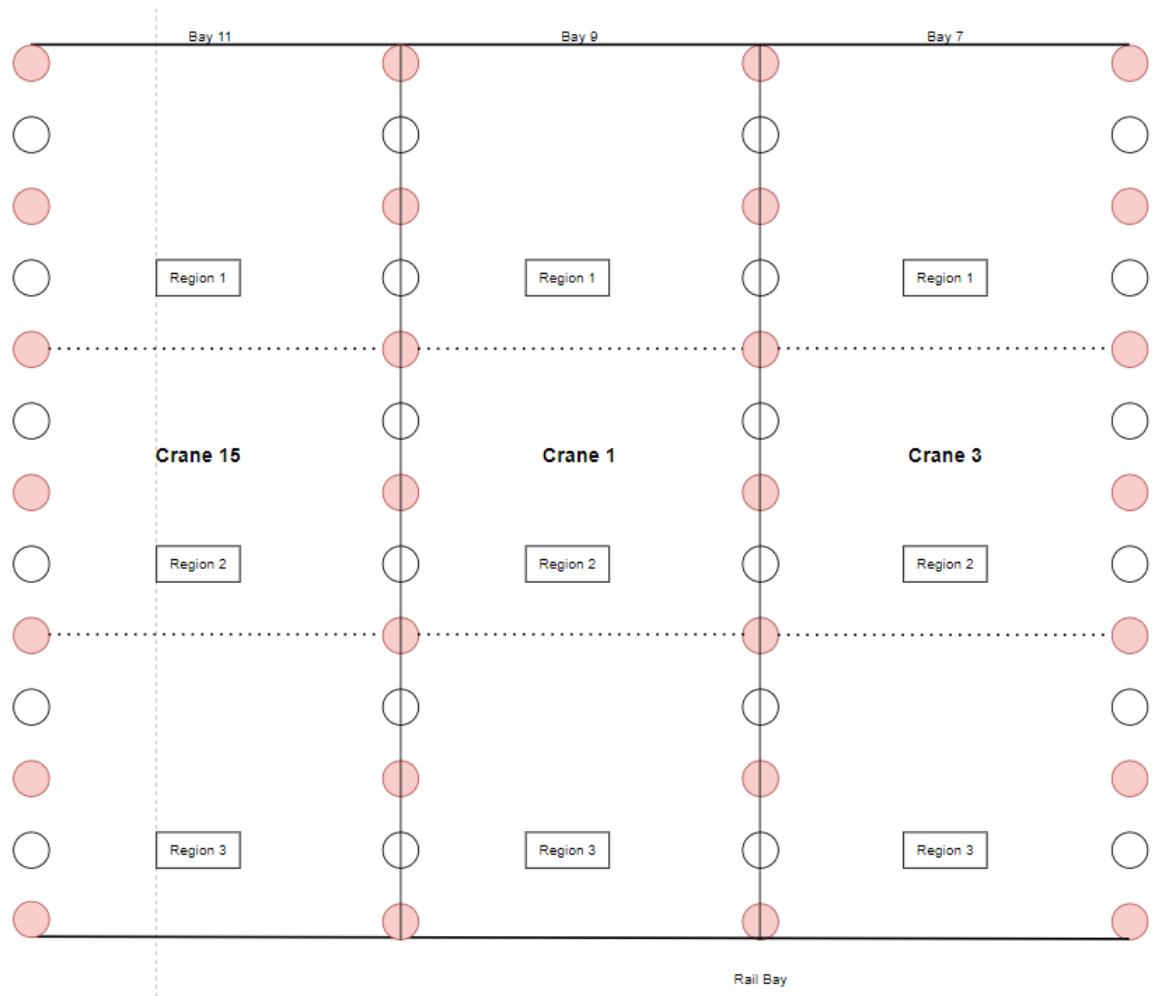


Figure 37: Expansion to Crane 1, 3 & 15